

R_K and R_{K^*} beyond the Standard Model

Gudrun Hiller^{1,*} and Ivan Nišandžić^{1,†}

¹*Institut für Physik, Technische Universität Dortmund, D-44221 Dortmund, Germany*

Measurements of the ratio of $B \rightarrow K^* \mu \mu$ to $B \rightarrow K^* e e$ branching fractions, R_{K^*} , by the LHCb collaboration strengthen the hints from previous studies with pseudoscalar kaons, R_K , for the breakdown of lepton universality, and therefore the Standard Model (SM), to $\sim 3.5\sigma$. Complementarity between R_K and R_{K^*} allows to pin down the Dirac structure of the new contributions to be predominantly SM-like chiral, with possible admixture of chirality-flipped contributions of up to $\mathcal{O}(\text{few}10\%)$. Scalar and vector leptoquark representations (S_3, V_1, V_3) plus possible (\tilde{S}_2, V_2) admixture can explain R_{K,K^*} via tree level exchange. Flavor models naturally predict leptoquark masses not exceeding a few TeV, with couplings to third generation quarks at $\mathcal{O}(0.1)$, implying that this scenario can be directly tested at the LHC.

Introduction. Gauge interactions of the leptons within the Standard Model (SM) exhibit exact universality. The only known source of lepton non-universality (LNU) are the Yukawa couplings of the leptons to the Higgs. Tests of lepton universality are provided by rare (semi)leptonic $|\Delta B| = |\Delta S| = 1$ transitions, which are induced in the SM at one loop and additionally suppressed by the Glashow-Iliopoulos-Maiani mechanism, therefore allowing to probe physics from scales significantly higher than the weak scale. Useful observables are the ratios of branching fractions of B meson decays into strange hadrons H and muon pairs over electron pairs [1]

$$R_H = \frac{\mathcal{B}(B \rightarrow H \mu^+ \mu^-)}{\mathcal{B}(B \rightarrow H e^+ e^-)}, \quad H = K, K^*, X_s, \dots \quad (1)$$

in which (lepton universal) hadronic effects cancel. The ratios are therefore predicted within the SM to be very close to one and provide a clean test of the SM [1].

The LHCb collaboration measured R_K in the dilepton invariant mass squared (q^2) bin $1 \text{ GeV}^2 \leq q^2 \leq 6 \text{ GeV}^2$ using the 1 fb^{-1} data set [2]

$$R_K^{\text{LHCb}} = 0.745_{-0.074}^{+0.090} \pm 0.036, \quad (2)$$

and, very recently, R_{K^*} within $1.1 \text{ GeV}^2 \leq q^2 \leq 6 \text{ GeV}^2$ [3]

$$R_{K^*}^{\text{LHCb}} = 0.69_{-0.07}^{+0.11} \pm 0.05, \quad (3)$$

with deviation from $R = 1$ by 2.6σ each. (Here and in the following we add statistical and systematic uncertainties in quadrature.) Corrections to $R = 1 + \mathcal{O}(m_\mu^2/m_B^2)$ [1] arise from electromagnetic interactions [4–7]. This affects the SM prediction at low q^2 at percent level [8], not qualitatively altering the fact that the data, (2) and (3) constitute a challenge to universality, and the SM.

Moreover, the importance of the measurement of R_{K^*} in addition to R_K is in its diagnosing power regarding different beyond the SM (BSM) contributions [9]. Left-handed and right-handed $b \rightarrow s$ currents enter $B \rightarrow K \ell \ell$ and $B \rightarrow K^* \ell \ell$ in almost orthogonal combinations in both regions of q^2 sensitive to LNU. Comparison of R_K with R_{K^*} , for instance through a double

ratio $X_{K^*} = R_{K^*}/R_K$ [9], probes directly right-handed LNU currents. The aim of this paper is to exploit this model-independently and pursue interpretations within leptoquark extensions of the SM.

Model-independent interpretation. We employ the usual effective Hamiltonian for $b \rightarrow s \ell \ell$, $\ell = e, \mu, \tau$ transitions

$$\mathcal{H}_{\text{eff}} = -\frac{4G_F \lambda_t}{\sqrt{2}} \frac{\alpha}{4\pi} \sum_i C_i^\ell \mathcal{O}_i^\ell + \text{h.c.}, \quad (4)$$

where $C_i^\ell, \mathcal{O}_i^\ell$ denote lepton-specific Wilson coefficients and dimension-six operators, respectively, renormalized at the scale $\mu \sim m_b$. Furthermore, G_F, α , and $\lambda_t = V_{tb}V_{ts}^*$ stand for Fermi's constant, the finestructure constant and the product of relevant Cabibbo-Kobayashi-Maskawa (CKM) matrix elements, respectively. The semileptonic operators read

$$\begin{aligned} \mathcal{O}_9^\ell &= (\bar{s} \gamma^\mu P_L b) (\bar{\ell} \gamma_\mu \ell), & \mathcal{O}_9^{\prime\ell} &= (\bar{s} \gamma^\mu P_R b) (\bar{\ell} \gamma_\mu \ell), \\ \mathcal{O}_{10}^\ell &= (\bar{s} \gamma^\mu P_L b) (\bar{\ell} \gamma_\mu \gamma_5 \ell), & \mathcal{O}_{10}^{\prime\ell} &= (\bar{s} \gamma^\mu P_R b) (\bar{\ell} \gamma_\mu \gamma_5 \ell), \end{aligned} \quad (5)$$

with chiral projectors $P_{L,R} = 1/2(1 \mp \gamma_5)$. The operators with chiral lepton currents,

$$\mathcal{O}_{AB}^\ell = (\bar{s} \gamma^\mu P_A b) (\bar{\ell} \gamma_\mu P_B \ell), \quad A, B = L, R, \quad (6)$$

are related to the $\mathcal{O}_{9,10}^{(\prime)\ell}$ as

$$\begin{aligned} C_9^\ell &= \frac{1}{2}(C_{LL}^\ell + C_{LR}^\ell), & C_{10}^\ell &= \frac{1}{2}(C_{LR}^\ell - C_{LL}^\ell), \\ C_9^{\prime\ell} &= \frac{1}{2}(C_{RL}^\ell + C_{RR}^\ell), & C_{10}^{\prime\ell} &= \frac{1}{2}(C_{RR}^\ell - C_{RL}^\ell). \end{aligned} \quad (7)$$

Within the SM the (lepton universal) Wilson coefficients are $C_9^{\text{SM}} = 4.07, C_{10}^{\text{SM}} \simeq -4.31$ [10], thus $C_{LL}^{\text{SM}} = C_9^{\text{SM}} - C_{10}^{\text{SM}} \simeq 8.4$, while scalar or tensor Wilson coefficients are negligible. We define $C_{LL}^\ell = C_{LL}^{\text{SM}} + C_{LL}^{\text{NP}\ell}$ [9] and drop the label "NP" (new physics) for Wilson coefficients negligible within the SM.

In the $B \rightarrow K^{(*)} \ell \ell$ branching fractions contributions from photon exchange enter, notably from charm loops

and dipole operators. These contributions are numerically small at high and low q^2 , sufficiently away from the photon pole, and lepton universal. Within current accuracy of R_{K,K^*} these contributions can be safely neglected. In this limit [9]

$$\begin{aligned} R_K &= 1 + \Delta_+ + \Sigma_+, \\ R_{K^*} &= 1 + \Delta_+ + \Sigma_+ + p(\Sigma_- - \Sigma_+ + \Delta_- - \Delta_+), \end{aligned} \quad (8)$$

where

$$\begin{aligned} \Delta_{\pm} &= 2\Re\left(\frac{C_{LL}^{\text{NP}\mu} \pm C_{RL}^{\mu}}{C_{LL}^{\text{SM}}} - (\mu \rightarrow e)\right), \\ \Sigma_{\pm} &= \frac{|C_{LL}^{\text{NP}\mu} \pm C_{RL}^{\mu}|^2 + |C_{LR}^{\mu} \pm C_{RR}^{\mu}|^2}{|C_{LL}^{\text{SM}}|^2} - (\mu \rightarrow e). \end{aligned} \quad (9)$$

Since BSM contributions in $|\Delta B| = |\Delta S| = 1$ transitions are smaller than the SM ones [10] the dominant BSM effect is captured by the linear (interference) terms Δ_{\pm} .

The coefficient p in Eq. (8) denotes the fraction of transverse parallel and longitudinal contributions to the $B \rightarrow K^* \ell \ell$ branching ratio [9]. Due to helicity arguments $p \sim 1$ both at low recoil (high q^2) and at low q^2 . Consequently, $\mathcal{B}(B \rightarrow K^* \ell \ell)$ is dominated by contributions proportional to $|C - C'|^2$. Since $\mathcal{B}(B \rightarrow K \ell \ell) \propto |C + C'|^2$ due to parity invariance of the strong interaction both modes are complementary and deviations of R_K from R_{K^*} probe primed operators [9].

Using (2),(3) one obtains

$$X_{K^*} = R_{K^*}/R_K = 0.94 \pm 0.18, \quad (10)$$

$$R_{K^*} + R_K - 2 = -0.54 \pm 0.14, \quad (11)$$

which gives, at 1σ

$$\Re[C_9^{\text{NP}\mu} - C_{10}^{\text{NP}\mu} - (\mu \rightarrow e)] \sim -1.1 \pm 0.3, \quad (12)$$

$$\Re[C_9^{\prime\mu} - C_{10}^{\prime\mu} - (\mu \rightarrow e)] \sim 0.1 \pm 0.4. \quad (13)$$

As anticipated, $|C^{\text{NP}}| \ll |C^{\text{SM}}|$. Therefore, the linear approximation, that is, neglecting the Σ_{\pm} -terms, is meaningful within the current experimental precision. Dropping quadratic terms greatly simplifies the interpretation of the data: Only BSM in O_{LL}^{ℓ} or O_{RL}^{ℓ} is able to explain R_{K,K^*} .

In Fig. 1 a χ^2 fit for the left- and right-handed Wilson coefficients is shown. The discrepancy with the SM is about $\sim 3.5\sigma$, where we allowed for a few percent deviations from $R = 1$ [8]. Interestingly, solutions with $C_9^{\text{NP}\mu} \sim -1$ are also favored by a global fit [10] to $b \rightarrow s\mu\mu$ observables. Taking this into account suggests an explanation of R_{K,K^*} anomalies with BSM predominantly residing in the muons.

Leptoquark explanations. We consider leptoquark extensions of the SM with tree level couplings to down-type quarks and leptons. Representations under

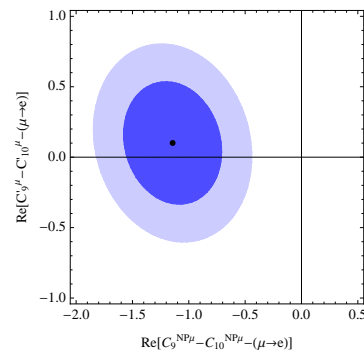


Figure 1: Fit of left- and light-handed BSM coefficients in $|\Delta B| = |\Delta S| = 1$ transitions to R_K and R_{K^*} data (2), (3). Darker and lighter shaded regions correspond to 68 and 95 % CL intervals, respectively.

	representation	C_{AB}	Relation	$R_{K^{(*)}}$
\tilde{S}_2	(3, 2, 1/6)	C_{RL}	$C_9' = -C_{10}'$	$R_K < 1, R_{K^*} > 1$
S_3	$(\bar{3}, 3, 1/3)$	C_{LL}^{NP}	$C_9 = -C_{10}$	$R_K \simeq R_{K^*} < 1$.
S_2	(3, 2, 7/6)	C_{LR}	$C_9 = C_{10}$	$R_K \simeq R_{K^*} \simeq 1$
\tilde{S}_1	$(\bar{3}, 1, 4/3)$	C_{RR}	$C_9' = C_{10}'$	$R_K \simeq R_{K^*} \simeq 1$

Table I: Scalar leptoquarks and relations between Wilson coefficients, assuming a single leptoquark at the time. The last column shows implications for R_{K^*} assuming $R_K < 1$, as suggested by data (2).

$SU(3)_C \times SU(2)_L \times U(1)_Y$ with relevant Wilson coefficients are given in Table I for scalar S_i^1 and in Table II for vector leptoquarks V_i , respectively. The index $i = 1, 2, 3$ refers to the dimension of the $SU(2)_L$ multiplet, see e.g. [11–13] for overviews.

The scalar leptoquarks S_2 and \tilde{S}_1 generate only C_{LR} and C_{RR} , respectively, which do not interfere with the SM contribution, see Eq. (9), and lead to R_K, R_{K^*} near 1. We therefore discard these two possibilities as explanations of the R_{K,K^*} anomalies.

In view of the experimental constraints shown in Fig. 1 we focus on leptoquarks that can give a sizable $C_{LL}^{\text{NP}\ell} = 2C_9^{\text{NP}\ell} = -2C_{10}^{\text{NP}\ell}$. This singles out the scalar triplet S_3 , the vector singlet V_1 and the vector triplet V_3 . This scalar and the vectors have been considered as a possible explanation of R_K (2) in [12, 14–17] and in [12, 17–21], respectively. Subdominant contributions from right-handed currents can be provided by additional leptoquarks \tilde{S}_2 or V_2 , which induce $C_{RL}^{\ell} = 2C_9^{\ell} = -2C_{10}^{\ell}$.

¹ In the literature the scalar leptoquarks S_2 and \tilde{S}_2 are also denoted by \tilde{R}_2 and \tilde{R}_2 , respectively.

	representation	C_{AB}	Relation	$R_{K^{(*)}}$
V_1	(3, 1, 2/3)	C_{LL}^{NP}	$C_9 = -C_{10}$	$R_K \simeq R_{K^*} < 1$
		C_{RR}	$C'_9 = +C'_{10}$	$R_K \simeq R_{K^*} \simeq 1$
V_2	(3, 2, -5/6)	C_{RL}	$C'_9 = -C'_{10}$	$R_K < 1, R_{K^*} > 1$
		C_{LR}	$C_9 = +C_{10}$	$R_K \simeq R_{K^*} \simeq 1$
V_3	(3, 3, -2/3)	C_{LL}^{NP}	$C_9 = -C_{10}$	$R_K \simeq R_{K^*} < 1$

Table II: Vector leptoquarks and implications for R_{K^*} assuming $R_K < 1$, as suggested by data (2), see Table I.

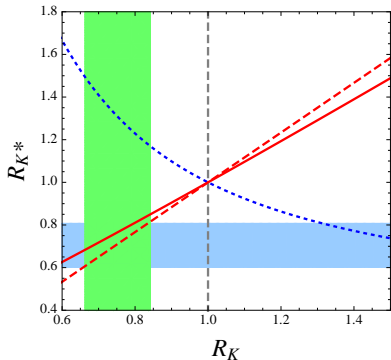


Figure 2: R_K versus R_{K^*} in BSM scenarios. Solid red curve: C_{LL}^{NP} ($C_9^{\text{NP}} = -C_{10}^{\text{NP}}$) corresponding to S_3, V_1 or V_3 , blue dotted curve: C_{RL} (\tilde{S}_2 or V_2), gray dashed curve: $C_{RL} = -C_{LL}^{\text{NP}}$ (no single leptoquark), and red dashed curve: C_{LL}^{NP} and $C_{RL} = -1/10 C_{LL}^{\text{NP}}$ (for instance, S_3 plus 10% admixture of \tilde{S}_2). The colored bands correspond to the LHCb measurements of R_K (2) and R_{K^*} (3).

In these models [12, 13]

$$C_{LL}^{\text{NP}\ell} = \frac{k_{LQ}\pi\sqrt{2}YY^*}{G_F\lambda_t\alpha} \frac{1}{M^2}, \quad k_{LQ} = 1, -1, -1 \text{ for } S_3, V_1, V_3, \quad (14)$$

$$C_{RL}^\ell = \frac{k_{LQ}\pi\sqrt{2}YY^*}{G_F\lambda_t\alpha} \frac{1}{M^2}, \quad k_{LQ} = -1/2, +1 \text{ for } \tilde{S}_2, V_2. \quad (15)$$

Here, M (Y) denotes the leptoquark mass (coupling).

Model-independent and leptoquark specific predictions for R_K versus R_{K^*} are shown in Fig. 2. The green and blue band denote the 1σ band of R_K (2) and R_{K^*} (3), respectively. Also shown are BSM scenarios which can (red solid and dashed lines) or cannot (blue dotted and gray dashed lines) simultaneously explain the data. Concretely, leptoquark \tilde{S}_2 , corresponding to the blue dotted curve, and which has been considered in the context of R_K [14, 22–24], is disfavoured as the sole source of LNU by the measurement of R_{K^*} . The numerics are based on the full expressions for the decay rates, for $\ell = \mu$. Recall, however, to linear approximation only non-universality matters.

We find for the dominant, SM-like chiral contribution

S_3

$$\frac{Y_{b\mu}Y_{s\mu}^* - Y_{be}Y_{se}^*}{M^2} \simeq \frac{1.1}{(35 \text{ TeV})^2}, \quad (S_3) \quad (16)$$

and similarly for V_1 or V_3 . To accommodate an admixture of right-handed currents we need contributions from another leptoquark, such as \tilde{S}_2

$$\frac{Y_{b\mu}Y_{s\mu}^* - Y_{be}Y_{se}^*}{M^2} \simeq \frac{-0.1}{(24 \text{ TeV})^2}. \quad (\tilde{S}_2) \quad (17)$$

Understanding the mass range is linked to flavor. The leptoquark coupling matrix Y is a 3×3 matrix in generation space, with rows corresponding to quark flavor and columns corresponding to lepton flavor. The presence of both kinds of fermions in one vertex is beneficial; it allows to probe flavor in new ways beyond SM fermion masses and mixings. Viable models are those employing a Froggatt-Nielsen $U(1)_{FN}$ to generate mass hierarchies for quarks and charged leptons together with a discrete, non-abelian group such as A_4 , which allows to accommodate neutrino properties [25, 26]. Applied to leptoquark models this allows to select lepton species – for instance having only couplings to one lepton species, muons, or electrons [16]. Corrections to lepton isolation arise from rotations to the mass basis and at higher order in the spurion expansion, and induce lepton flavor violation [12, 16, 27–30] such as $B \rightarrow K\mu\tau$, which can be probed with B -physics experiments but also $\mu - e$ -conversion, rare K and $\ell \rightarrow \ell'$ decays. Together with $B \rightarrow K^{(*)}\nu\bar{\nu}$ modes the latter constitute the leading constraints on flavor models and LNU anomalies, and improved experimental study is promising.

A generic prediction for S_3, V_1, V_3 – all of them couple quark doublets to lepton doublets – is obtained from simple flavor patterns such as ℓ -isolation, $\ell = e, \mu$, [12, 16]

$$Y_{q_3\ell} \sim c_\ell, \quad Y_{q_2\ell} \sim c_\ell\lambda^2, \quad q_3 = b, t, \quad q_2 = s, c, \quad (18)$$

where $c_\ell \sim \lambda \sim 0.2$. Note that the FN-mechanism is only able to explain parametric suppressions in specific powers of the parameter λ up to numbers of order one. Irrespective of the concrete flavor symmetry, each coupling Y to lepton doublets brings in a non-abelian spurion insertion suppression, the factor c_ℓ , which is unavoidable as lepton doublets are necessarily charged under the non-abelian group to obtain a viable PMNS-matrix. The suppression of the additional couplings to right-handed leptons in $V_{1,2}$ can be achieved using flavor symmetries [12, 20].

Putting lepton and neutrino properties aside, a minimal prediction is $Y_{s\ell}/Y_{b\ell} \sim m_s/m_b$, hence $Y_{b\ell}Y_{s\ell}^* \sim \lambda^2 \simeq \text{few} \times 0.01$. Eq. (16) implies $M \sim 5 - 10$ TeV, accessible at the LHC at least partly with single production.

Eq. (18) points to lower values of leptoquark masses, see Fig. 3. Also shown are constraints from $B_s - \bar{B}_s$ mixing, induced at one loop through box diagrams and

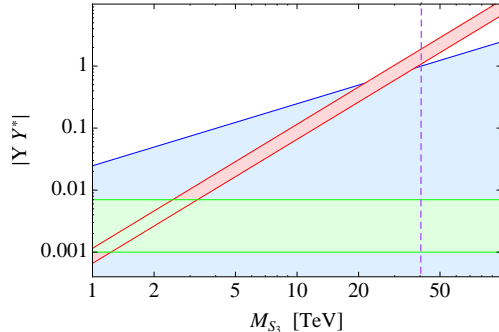


Figure 3: Allowed values of $|YY^*|, M_{S_3}$ by Δm_{B_s} (blue area) and $R_{K^{(*)}}$ (red band) (12). The green band corresponds to flavor model predictions (18). The dashed blue line corresponds to the upper limit on the mass of the S_3 leptoquark (19).

which constrains the *square* of YY^* over M^2 [14]. A data-driven upper limit, irrespective of flavor, is obtained as

$$M \lesssim 40 \text{ TeV}, 45 \text{ TeV}, 20 \text{ TeV} \quad \text{for } S_3, V_1, V_3. \quad (19)$$

We assume vector leptoquarks to be gauge-like and employ the usual Hamiltonian

$$\mathcal{H}_{\text{eff}}^{\Delta B=2} = (C_1^{SM} + C_1^{LQ})(\bar{b}\gamma_\mu(1-\gamma_5)s)(\bar{b}\gamma_\mu(1-\gamma_5)s) + \text{h.c.} \quad (20)$$

where

$$C_1^{LQ} = \frac{p_{LQ}(YY^*)^2}{128\pi^2 M^2}, \quad p_{LQ} = 5, 4, 20 \text{ for } S_3, V_1, V_3, \quad (21)$$

see, *e.g.* [31]. In general, $(YY^*)^2 \rightarrow \sum_{\ell_i, \ell_j} (Y_{b\ell_i} Y_{s\ell_i}^*)(Y_{b\ell_j} Y_{s\ell_j}^*)$. It follows that

$$\Delta m_{B_s}^{LQ} / \Delta m_{B_s}^{SM} = \frac{p_{LQ}(YY^*)^2}{8M^2 G_F^2 m_W^2 \lambda_t^2 S_0(x_t)}, \quad (22)$$

where S_0 is an Inami-Lim function, $x_t = m_t^2/m_W^2$. We use $\Delta m_{B_s}^{exp} / \Delta m_{B_s}^{SM} = 1.02 \pm 0.10$ [28, 32].

Direct limits for scalar leptoquarks decaying 100 % into a muon (electron) and a jet are $M > 1050 \text{ GeV}$ [33] ($M > 1755 \text{ GeV}$ [34]). For vector leptoquarks, the limits are model-dependent and read $M > 1200 - 1720 \text{ GeV}$ ($M > 1150 - 1660 \text{ GeV}$) for 100 % decays to muon (electron) plus jet [35]. The bounds weaken if decays into neutrinos are taken into account.

UV considerations. The main challenge for embedding light scalar leptoquarks into (complete) short-distance models is proton decay. From Table I only S_2, \tilde{S}_2 do not couple to quark bilinears ($\bar{q}q$) and, thus, do not induce proton decay at tree-level. In addition, dangerous couplings to the Higgs doublet should be suppressed [13, 36].

SM gauge-invariance allows S_3 to couple to quark bilinears

$$\mathcal{L}_{QQ} = Y_\kappa \bar{Q}_L^C \alpha (i\sigma^2)^{\alpha\beta} (S_3^\dagger)^{\beta\gamma} Q_L^\gamma + \text{h.c.}, \quad (23)$$

with isospin indices α, β, γ . The Yukawa coupling Y_κ is anti-symmetric in flavor space [37, 38], thus S_3 does not introduce proton decay at tree level, however, couplings to $ut(c)$ can induce the process via higher orders diagrams [38].

Within flavor models, the dangerous terms in (23) receive suppressions. For $U(1)_{FN} \times A_4 \times Z_3$, and assuming that the quarks transform trivially under A_4 , we find that this requires at least 2 spurion fields ξ and ξ' , see [16] for details. Including the FN-suppression for the up-quark this amounts to $\lambda^4 \kappa \kappa' \lesssim 10^{-4}$. Viable patterns for R_K are obtained with second generation quarks in non-trivial representations of A_4 . This way, however, the ut coupling cannot be suppressed further.

If the evidence for LNU in C_{LL}^{NP} strengthens, it would be important to understand the origin of the leptoquark S_3 which provides an explicit high-energy realization. One possibility was suggested in Ref. [15]. The S_3 appears, along with the Higgs doublet, as a pseudo-Goldstone boson of the strong dynamics around TeV scale, while the proton decay is avoided with a discrete symmetry.

An alternative possibility is to trace the origin of S_3 to a Grand Unified Theory (GUT). The S_3 is contained in the $\mathbb{1}\bar{26}_H$ scalar multiplet of $SO(10)$ [13, 39]. The dangerous couplings to quark bilinears are forbidden by $SO(10)$ -invariance - the corresponding Yukawa coupling to fermion multiplets is $y_{ij} 16_i 16_j \mathbb{1}\bar{26}_H$ which embeds only the couplings to leptons and quarks, but not to quark bilinears. The 16_i denotes the spinor representation of $SO(10)$ that unifies all SM fermions of a single generation and a right-handed neutrino, and $i = 1, 2, 3$ is a flavor index. The S_3 might play a role in correcting the phenomenologically unsuccessful prediction of the relation between the mass matrices of down-type quarks and charged leptons in the minimal $SU(5)$ [40, 41].

Vector leptoquarks appear as super-heavy gauge bosons in a GUT, with masses near the unification scale. For example, the state with quantum numbers of V_1 is a gauge boson in models of quark-lepton unification, *e.g.* the original Pati-Salam model or variants thereof, see [42]. V_1, V_3 do not couple to quark bilinears and are safe with regards to proton decay. If V_1 is a gauge boson, the corresponding left- and right-handed couplings are unitary. It is then more difficult to suppress the unwanted (right-handed) couplings and simultaneously avoid the constraints from the first generation fermions. The embedding of V_3 into a UV complete model is challenging [43].

The low scale non-gauge spin-1 leptoquarks might be obtained as composite states from strongly coupled dynamics, in which case they are accompanied by other composite states.

Conclusions. The recent measurement of R_{K^*} (3) by the LHCb collaboration challenges lepton universality, an inbuilt feature of the SM and many of its extensions,

further: combined with R_K (2) the discrepancy with the SM is $\sim 3.5\sigma$. The LNU contributions to $|\Delta B| = |\Delta S| = 1$ FCNCs are predominantly SM-like chiral, with possible admixture of right-handed contributions up to the order of few 10%, see Fig. 1. Since R_K and R_{K^*} suffice to determine the chiral structure, measurements of further LNU ratios R_H into different final states and angular distributions [9, 44] provide consistency checks. Using R_{K,K^*} data we predict the ratio of inclusive $B \rightarrow X_s \ell \ell$ branching fractions

$$R_{X_s} \sim 0.73 \pm 0.07, \quad (24)$$

consistent with earlier findings by Belle $R_{X_s} = 0.42 \pm 0.25$ [45] and BaBar $R_{X_s} = 0.58 \pm 0.19$ [46]².

Leptoquarks naturally induce LNU in semileptonic decays at tree level. The scalar S_3 and the vector $V_{1,3}$ representations can account for the dominant, SM-like chiral contribution (12). Their masses are limited to not exceed the multi-10 TeV range in order to comply with data, see (19) for details. Leptoquark explanations of R_{K,K^*} within flavor models, which simultaneously address the masses and mixings of SM fermions require leptoquark masses in the few TeV-region, which can be explored at the LHC, see Fig. 3. The dominant decay modes of the triplets S_3 and V_3 are $b\mu, t\mu, b\nu$ and $t\nu$, whereas the $SU(2)_L$ -singlet V_1 decays predominantly to $b\mu, t\nu$. The respective Yukawa couplings are at the level $O(0.1)$. Ignoring the pull from the global fit to $b \rightarrow s\mu\mu$ LNU can also stem from sizable BSM contributions to $b \rightarrow see$. In this case modes into final state electrons (and corresponding neutrinos) are dominant.

Acknowledgements. This project is supported in part by the Bundesministerium für Bildung und Forschung (BMBF). We thank Ivo de Medeiros Varzielas for useful discussions.

* Electronic address: gkiller@physik.uni-dortmund.de

† Electronic address: ivan.nisandzic@tu-dortmund.de

- [1] G. Hiller and F. Krüger, Phys. Rev. D **69** (2004) 074020 [[hep-ph/0310219](#)].
 [2] R. Aaij *et al.* [LHCb Collaboration], Phys. Rev. Lett. **113** (2014) 151601 [[arXiv:1406.6482](#) [hep-ex]].
 [3] R. Aaij *et al.* [LHCb Collaboration], [arXiv:1705.05802](#) [hep-ex].
 [4] T. Huber, E. Lunghi, M. Misiak and D. Wyler, Nucl. Phys. B **740**, 105 (2006) [[hep-ph/0512066](#)].
 [5] C. Bobeth, G. Hiller and G. Piranishvili, JHEP **0712**, 040 (2007) [[arXiv:0709.4174](#) [hep-ph]].

- [6] T. Huber, T. Hurth and E. Lunghi, Nucl. Phys. B **802**, 40 (2008) doi:10.1016/j.nuclphysb.2008.04.028 [[arXiv:0712.3009](#) [hep-ph]].
 [7] T. Huber, T. Hurth and E. Lunghi, JHEP **1506**, 176 (2015) doi:10.1007/JHEP06(2015)176 [[arXiv:1503.04849](#) [hep-ph]].
 [8] M. Bordone, G. Isidori and A. Pattori, Eur. Phys. J. C **76**, no. 8, 440 (2016) [[arXiv:1605.07633](#) [hep-ph]].
 [9] G. Hiller and M. Schmaltz, JHEP **1502** (2015) 055 [[arXiv:1411.4773](#) [hep-ph]].
 [10] S. Descotes-Genon, L. Hofer, J. Matias and J. Virto, JHEP **1606** (2016) 092 [[arXiv:1510.04239](#) [hep-ph]].
 T. Hurth, F. Mahmoudi and S. Neshatpour, JHEP **1412** (2014) 053 [[arXiv:1410.4545](#) [hep-ph]].
 W. Altmannshofer and D. M. Straub, Eur. Phys. J. C **75** (2015) no.8, 382 [[arXiv:1411.3161](#) [hep-ph]].
 F. Beaujean, C. Bobeth and D. van Dyk, Eur. Phys. J. C **74** (2014) 2897 Erratum: [Eur. Phys. J. C **74** (2014) 3179] [[arXiv:1310.2478](#) [hep-ph]].
 [11] N. Košnik, Phys. Rev. D **86** (2012) 055004 [[arXiv:1206.2970](#) [hep-ph]].
 [12] G. Hiller, D. Loose and K. Schönwald, JHEP **1612** (2016) 027 [[arXiv:1609.08895](#) [hep-ph]].
 [13] I. Doršner, S. Fajfer, A. Greljo, J. F. Kamenik and N. Košnik, Phys. Rept. **641** (2016) 1 [[arXiv:1603.04993](#) [hep-ph]].
 [14] G. Hiller and M. Schmaltz, Phys. Rev. D **90** (2014) 054014 [[arXiv:1408.1627](#) [hep-ph]].
 [15] B. Gripaios, M. Nardecchia and S. A. Renner, JHEP **1505** (2015) 006 [[arXiv:1412.1791](#) [hep-ph]].
 [16] I. de Medeiros Varzielas and G. Hiller, JHEP **1506** (2015) 072 [[arXiv:1503.01084](#) [hep-ph]].
 [17] R. Barbieri, G. Isidori, A. Pattori and F. Senia, Eur. Phys. J. C **76**, no. 2, 67 (2016) doi:10.1140/epjc/s10052-016-3905-3 [[arXiv:1512.01560](#) [hep-ph]].
 [18] S. Fajfer and N. Konik, Phys. Lett. B **755** (2016) 270 [[arXiv:1511.06024](#) [hep-ph]].
 [19] D. Bečirević, N. Košnik, O. Sumensari and R. Zukanovich Funchal, JHEP **1611** (2016) 035 [[arXiv:1608.07583](#) [hep-ph]].
 [20] R. Alonso, B. Grinstein and J. Martin Camalich, JHEP **1510** (2015) 184 [[arXiv:1505.05164](#) [hep-ph]].
 [21] L. Calibbi, A. Crivellin and T. Ota, Phys. Rev. Lett. **115** (2015) 181801 [[arXiv:1506.02661](#) [hep-ph]].
 [22] S. Sahoo and R. Mohanta, Phys. Rev. D **91**, no. 9, 094019 (2015) doi:10.1103/PhysRevD.91.094019 [[arXiv:1501.05193](#) [hep-ph]].
 [23] D. Bečirević, S. Fajfer and N. Košnik, Phys. Rev. D **92** (2015) no.1, 014016 [[arXiv:1503.09024](#) [hep-ph]].
 [24] P. Cox, A. Kusenko, O. Sumensari and T. T. Yanagida, JHEP **1703**, 035 (2017) doi:10.1007/JHEP03(2017)035 [[arXiv:1612.03923](#) [hep-ph]].
 [25] G. Altarelli and F. Feruglio, Rev. Mod. Phys. **82**, 2701 (2010) [[arXiv:1002.0211](#) [hep-ph]].
 [26] I. de Medeiros Varzielas and L. Merlo, JHEP **1102**, 062 (2011) [[arXiv:1011.6662](#) [hep-ph]].
 [27] S. L. Glashow, D. Guadagnoli and K. Lane, Phys. Rev. Lett. **114** (2015) 091801 [[arXiv:1411.0565](#) [hep-ph]].
 [28] D. Bečirević, O. Sumensari and R. Zukanovich Funchal, Eur. Phys. J. C **76** (2016) no.3, 134 [[arXiv:1602.00881](#) [hep-ph]].
 [29] M. Duraisamy, S. Sahoo and R. Mohanta, Phys. Rev. D **95**, no. 3, 035022 (2017) doi:10.1103/PhysRevD.95.035022 [[arXiv:1610.00902](#)]

² The BaBar collaboration finds an excess of electrons relative to the SM prediction, especially in the lowest q^2 -bin.

- [hep-ph].
- [30] A. Crivellin, D. Müller and T. Ota, [arXiv:1703.09226](#) [hep-ph].
- [31] S. Davidson, D. C. Bailey and B. A. Campbell, *Z. Phys. C* **61** (1994) 613 [[hep-ph/9309310](#)].
- [32] C. Patrignani *et al.* [Particle Data Group], *Chin. Phys. C* **40** (2016) no.10, 100001.
- [33] M. Aaboud *et al.* [ATLAS Collaboration], *New J. Phys.* **18**, no. 9, 093016 (2016) [[arXiv:1605.06035](#) [hep-ex]].
- [34] V. Khachatryan *et al.* [CMS Collaboration], *Phys. Rev. D* **93**, no. 3, 032005 (2016) [[arXiv:1509.03750](#) [hep-ex]].
- [35] V. Khachatryan *et al.* [CMS Collaboration], *Phys. Rev. D* **93**, no. 3, 032004 (2016) [[arXiv:1509.03744](#) [hep-ex]].
- [36] J. M. Arnold, B. Fornal and M. B. Wise, *Phys. Rev. D* **87** (2013) 075004 [[arXiv:1212.4556](#) [hep-ph]].
- [37] L. Vecchi, *JHEP* **1110** (2011) 003 [[arXiv:1107.2933](#) [hep-ph]].
- [38] I. Doršner, S. Fajfer and N. Košnik, *Phys. Rev. D* **86** (2012) 015013 [[arXiv:1204.0674](#) [hep-ph]].
- [39] R. Slansky, *Phys. Rept.* **79** (1981) 1.
- [40] H. Georgi and S. L. Glashow, *Phys. Rev. Lett.* **32** (1974) 438.
- [41] H. Georgi and C. Jarlskog, *Phys. Lett.* **86B** (1979) 297.
- [42] P. Fileviez Perez and M. B. Wise, *Phys. Rev. D* **88** (2013) 057703 [[arXiv:1307.6213](#) [hep-ph]].
- [43] C. Biggio, M. Bordone, L. Di Luzio and G. Ridolfi, *JHEP* **1610** (2016) 002 [[arXiv:1607.07621](#) [hep-ph]].
- [44] S. Wehle *et al.* [Belle Collaboration], *Phys. Rev. Lett.* **118**, no. 11, 111801 (2017) [[arXiv:1612.05014](#) [hep-ex]].
- [45] Toru Iijima, for the Belle collaboration, Talk at the XXIV International Symposium on Lepton Photon Interactions at High Energies (Lepton-Photon 2009), August 17-22, 2009, Hamburg, Germany.
- [46] J. P. Lees *et al.* [BaBar Collaboration], *Phys. Rev. Lett.* **112**, 211802 (2014) [[arXiv:1312.5364](#) [hep-ex]].